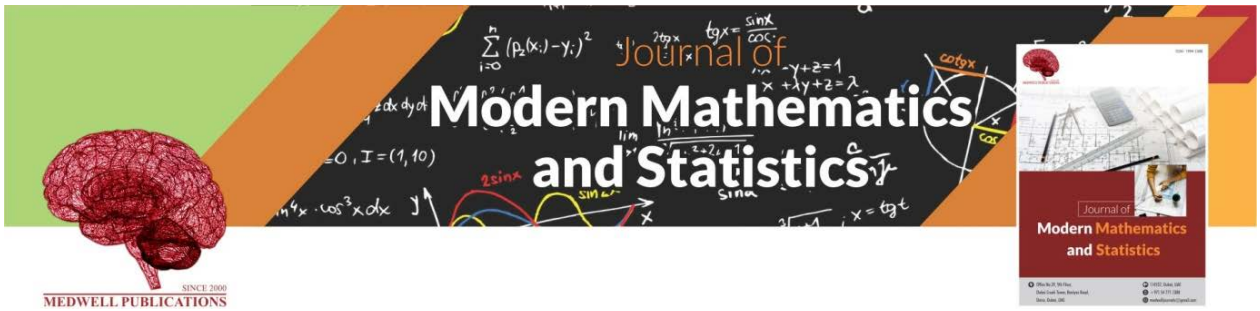

Modified Mathematical Model on the Study of Convective MHD Nanofluid Flow with Heat Generation/Absorption along with Thermophoresis and Brownian Motion on Boundary Layer Flow over a Linearly Stretching Sheet

Abdul. G. Madaki and A.A. Hussaini
Department of Mathematical Sciences, Abubakar Tafawa Balewa University, Bauchi, Nigeria

Key words: Heat generation/absorption, Boundary-layer, Brownian motion, Nanofluid, Stretching sheet, Thermophoresis

Corresponding Author:
Abdul. G. Madaki
Department of Mathematical Sciences, Abubakar Tafawa Balewa University, Bauchi, Nigeria

Page No.: 39-46
Volume: 15, Issue 3, 2021
ISSN: 1994-5388
Journal of Modern Mathematics and Statistics

Abstract: A numerical investigation is presented to show the effects of convective nanofluid flow with heat generation/absorption over a linearly stretching sheet by considering thermophoresis and Brownian motion in the presence of heat generation/absorption. A suitable set of similarity transformations are used together with the boundary conditions in order to convert the basic partial differential equations into a set of corresponding nonlinear ordinary differential equations. Runge-Kutta-Fehlberg method along with shooting technique is involved in order to solve the reduced governing basic equations. The influences of several emerging physical parameters of nanofluid on the profiles of velocity, temperature and nanoparticle volume fraction, Nusselt number and Sherwood number have been studied and analyzed in detail through graphs and tables. It is noticed that, the reduced Sherwood number is a decreasing function with both heat generation/absorption parameters. It is also noticed that the Brownian motion and thermophoresis parameter have the reverse effects on nanofluid Sherwood number. It is analyzed that the Nusselt number decreases with an increase in the values of thermophoresis parameter, Brownian motion parameter. It is observed that the Sherwood number has ascending behavior for thermophoresis and Brownian motion parameters whereas nanofluid Sherwood number gets amplified with a hike for all the values of Brownian motion parameter.

INTRODUCTION

Many pieces of research have been carried out on the notion behind the heat transfer enhancement by using nanofluids. Choi[1] was the first Scientist to coined nanofluid in his bid to propose the new class of enhancing heat transfer fluid by dispersing nano-sized particles in a base fluid. The fluid flow over a stretching surface is indeed an essential and interesting case in engineering and sciences with an application such as metal spinning, wire drawing, extrusion and rubber sheets manufacturing among others. The convective heat transfer in nanofluids

is an amazing area of interest for many researchers for its wide purview of application in both sciences and engineering. The radiative effects in the nanofluid flow due to solar energy wasinvestigated by Mushtaq *et al*.[2]. Among other vital studies concerning the convective boundary layer flow are Aziz *et al*.[3].

Some recent studies, concerning the natural phenomenon of nanofluids have been investigated by Madaki *et al*.[4]. Furthermore, Pal and Mandal[5] investigated the hydromagnetic convective-radiative boundary layer flow of nanofluids caused by a non-linear vertical stretching/shrinking sheet with viscous dissipation numerically.

The term boundary layer flow is the fluid's flow region of a viscous fluid which is in the proximity of a body or a solid surface in contact with the fluid and in motion corresponding to the fluid. Very recently, Khazayinejad *et al*.[6] studied the boundary-layer flow of a nanofluid past a porous moving semi-infinite plate using an optimal collocation method.

The magnetohydrodynamic (MHD) nanofluid flows, being an electrically-conducting fluid have received a significant consideration due to its wide application in industrial technology such as high temperature plasmas and purification of molten metals from non-metallic inclusions in metallurgy by the application of a magnetic field[7].

The chemical reaction is quite a major platform required by many industrial applications in the manufacturing process. Naramgari and Sulochana studied the effects of both thermal radiation and chemical reaction on MHD flow over a permeable stretching/shrinking sheet of a nanofluid with suction/ injection. Recently, many researchers such as Animasaun[8] and Kasmani *et al*.[9] had all made a fantastic effort in studying the effects of chemical reaction in relation to various cases in sciences.

An analysis on the natural convective boundary layer flow, heat and mass transfer of nanofluid over a stretching sheet with convective boundary condition being the main mechanism was carried out by Madaki *et al*.[10].

In this study, our prime goal is to analyze the effect of heat generation/absorption on the above model. Some useful dimensionless quantities are used to transform the governing equations into ordinary differential equations. Both analytical and numerical techniques were used to derive the solution to the stated problem. The effect of heat generation/absorption along with all related parameters is investigated and presented in tabular and graphical forms, respectively.

MATERIALS AND METHODS

Problem formulation: We considered the two-dimensional (x, y) incompressible boundary-layer flow of

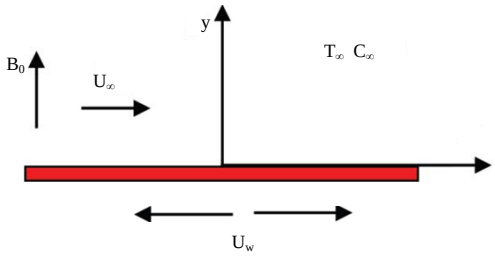

Fig. 1: Geometry of the problem

a nanofluid past a heated stretching sheet situated at y = 0 with convective boundary condition. The two equal and opposite forces from the origin are the directions where the sheet is stretched along x-axis and perpendicular to y-axis. The velocity at the sheet surface (wall) is kept at the fixed origin along the distance x, i.e., Uw = ax where a>0 and x is the coordinate along the sheet where the sheet velocity is zero as shown in Fig. 1.

Let the fluid's free stream velocity be U∞(x) = bx. The transverse magnetic field is subjected to the flow along y>0 normal to the fluid flow direction. Assume that, the external electrical field is zero while the electrical field caused by the polarization of charges is negligible. Then the mass transfer analysis is performed subject to heat generation/absorption as well as the other pertinent parameters effects. At the convective heating process, the sheet surface temperature T_w goes with quiescent fluid temperature T_f. The ambient fluid's temperature is denoted by T_∞. The nanoparticle concentration is denoted by C while C_w is the nanoparticle concentration at the wall and C_∞ is the ambient concentration.

These are the governing equations for the conservation of Momentum, Temperature and nanoparticle concentration based on the usual boundary layer assumptions, in the presence of Heat generation/absorption:

$$\frac{\partial\Psi}{\partial y}\frac{\partial^2\Psi}{\partial x\partial y}-\frac{\partial\Psi}{\partial x}\frac{\partial^2\Psi}{\partial y^2}=U_\infty\frac{\partial U_\infty}{\partial x}+\nu_f\frac{\partial^3\Psi}{\partial y^3}+\frac{\sigma_e B_0^2}{\rho_f}(u-U_\infty) \quad (1)$$

$$\frac{\partial\Psi}{\partial y}\frac{\partial T}{\partial x}-\frac{\partial\Psi}{\partial x}\frac{\partial T}{\partial y}=\alpha\frac{\partial^2 T}{\partial y^2}+\frac{\nu_f}{C_f}\left(\frac{\partial^2\Psi}{\partial y^2}\right)^2+\frac{\sigma_e B_0^2}{(\rho C)_f}(U_\infty-u)^2+\tau\left\{D_B\frac{\partial T}{\partial y}\frac{\partial C}{\partial y}+\frac{D_T}{T_\infty}\left(\frac{\partial T}{\partial y}\right)^2\right\}+\frac{16\sigma^* T^3}{3(\rho C)_f k^*}\frac{\partial^2 T}{\partial y^2}+\frac{Q}{\rho_{nf}}(T-T_\infty) \quad (2)$$

$$\frac{\partial\Psi}{\partial y}\frac{\partial C}{\partial x}-\frac{\partial\Psi}{\partial x}\frac{\partial C}{\partial y}=D_B\frac{\partial^2 C}{\partial y^2}+\frac{D_T}{T_\infty}\frac{\partial^2 T}{\partial y^2}-K_1(C-C_\infty) \quad (3)$$

Subject to the following boundary conditions:

$$\text{at } y=0: u=U_w(x)=ax, v=0, -k\frac{\partial T}{\partial y}=h(T_f-T), C=C_w.$$
$$\text{as } y\to\infty: u\to U_\infty(x)=bx, v=0, T=T_\infty, C=C_\infty \quad (4)$$

Here, the stream function $\Psi(x, y)$ is considered as $u = \partial\Psi/\partial y$, $v = -\partial\Psi/\partial x$ where, u and v are the velocities in x and y directions, U_∞ = is the free stream velocity, v_f is the kinematic viscosity of the fluid σ_e is the electrical conductivity, B_0 is the magnetic field, ρ_f the density of the nanofluid, T is the temperature, $(\rho C)_f$ is the heat capacity of the base fluid, ρ is the density, α is the thermal diffusivity, C_f is the skin friction coefficient of the fluid, D_B is the Brownian diffusion, DT is the thermophoretic diffusion, k_1 is the rate of chemical reaction, $\tau = (\rho C)_p/(\rho C)_f$ is the ratios of the effective heat capacity of the nanoparticle material to the heat capacity of the fluid, qris the radiative heat flux, k is the thermal conductivity of base fluid, h is the convective heat transfer coefficient and a and b are constants. The Rosseland approximation (1931) is used to evaluate the radiative heat flux in energy equation as:

$$q_r = -\frac{4\sigma^*\partial T^4}{3k^*\partial y}$$

where, σ^* and k^* are the Stefan-Boltzmann constant and the mean absorption number. The temperature variation amidst the flow is significantly limited and the expression $T^4 = 4T_\infty^3 T - 3T_\infty^4$ is considered in the energy equation as a linear function of temperature by using Taylor series expansion about T∞ and by ignoring the higher-order terms. We now introduce the following dimensionless quantities:

$$\eta = y\sqrt{\frac{a}{v_f}},\ \Psi = xf(\eta)\sqrt{av_f},\ u = axf'(\eta),\ v = f(\eta)\sqrt{av_f},\ \theta(\eta) = \frac{T-T_\infty}{T_f-T_\infty},\ T = \theta T_w,\ \phi(\eta) = \frac{C-C_\infty}{C_w-C_\infty},\ C = \phi C_w \tag{5}$$

Using the dimensionless quantities in Eq. 5 into Eq. 1-4, to obtain the following transformed ordinary differential equations:

$$f''' + ff'' - f'^2 + A^2 + M(A - f') = 0 \tag{6}$$

$$\left\{\left[1 + N\{1 + (\theta_c - 1)\theta\}^3\right]\theta'\right\}' + \Pr\left[f\theta' + Nb\theta'\phi' + Nt\theta'^2 + Ecf''^2 + MEc\left(\frac{b}{a} - f'\right)^2 + \lambda\theta\right] = 0 \tag{7}$$

$$\phi'' + Lef\phi' + \frac{Nt}{Nb}\theta'' - \gamma\phi = 0 \tag{8}$$

where, prime represents differentiation with respect to the function η, $M = \sigma_e B^2_0/a\rho_f$ is the magnetic parameter, A = b/a is the ratio of the rates of free stream velocity to the velocity of the stretching sheet, $N = 16\sigma^* T_4/3kk^*$ is the radiation parameter and $Pr = v_f/\alpha$ is the Prandtl number, $\lambda = Q/aT_w\rho_{nf}$ is the heat generation/absorption parameter. Here, the dimensionless temperature in Eq. 5 is written in the form $T = T_\infty(1+(\theta_c-1)\theta)$ where, $\theta_c = T_f/T_\infty$ Considering the first and the last terms on the right-hand side of Eq. 9, we, therefore, write:

$$\alpha\left(\frac{\partial}{\partial y}\right)\left[\frac{\partial T}{\partial y}\left(1 + N(1 + (\theta_c - 1)\theta)^3\right)\right] = \frac{a(T_f - T_\infty)}{Pr}[(1 + N(1 + (\theta_c - 1)\theta)^3)\theta']' \tag{9}$$

Equation 6-9 are subject to the following boundary conditions:

$$f(0) = 0, f'(\infty) = A, f'(0) = 1,\ \theta'(0) = -Bi[1 - \theta(0)],\ \theta(\infty) = 0,\ \phi(0) = 1,\ \phi(\infty) = 0 \tag{10}$$

The parameters involved in Eq. 6-11 are defined as follows:

$$Le = \frac{v_f}{D_B},\ Nb = \frac{\tau D_B(C_w - C_\infty)}{v_f},\ Nt = \frac{\tau D_B(T_f - T_\infty)}{v_f T_\infty},\ Bi = \frac{h(v_f/a)^{1/2}}{k},\ Ec = \frac{U_w^2(x)}{C_n(T_w - T_\infty)},\ \gamma = \frac{k_1 v_f(C_w - C_\infty)}{aD_B C_w}.$$

Here, Le is the Lewis number, Nb is the Brownian motion parameter, Nt is the thermophoresis parameter, Bi is the Biot number, Ec is the Eckert number γ and is the chemical reaction parameter. The quantities of practical interest are the Nusselt number, Nu and the Sherwood number, Sh. As we observed that *x*-coordinate does not fit to be ignored from the temperature equation. Therefore, we strive for the possible local similarity solutions. With q_w and qm being the wall heat flux and wall mass flux, respectively are given as follows:

$$q_w = -k\left(\frac{\partial T}{\partial y}\right)_{y=0} + (q_r)_w = -k(T_w - T_\infty)(a/v_f)^{1/2}[1 + N\theta_c^3]\theta'(0),\ q_m = -D_B\left(\frac{\partial C}{\partial y}\right)_{y=0} = -D_B(C_w - C_\infty)(a/v_f)^{1/2}\phi'(0) \tag{11}$$

Using the expressions of both local Nusselt and Sherwood numbers as:

$$Nu_x = \frac{xq_w}{k(T_w - T_\infty)} \Rightarrow -\sqrt{Re_x}[1 + N\theta_c^3]\theta'(0) = Nur,\ Sh = \frac{xq_m}{D_B(C_w - C_\infty)} \Rightarrow -\sqrt{Re_x}\ \phi'(0) = Shr \tag{12}$$

RESULTS AND DISCUSSION

An efficient fourth order Runge-Kutta method along with shooting technique has been employed to study the

Table 1: Comparison of values of reduced Nusselt number, (Nur) -θ'(0), reduced Sherwood number, (Shr) -φ'(0) with Madaki *et al.*[10] when Nt = Nb = 0.5 and R = γ = 0

			Madaki *et al.*[10]		Present study	
Pr	Bi	Le	-θ' (0)	-φ' (0)	-θ' (0)	-φ' (0)
1	0.1	5	0.07892	1.5476	0.07892	1.5476
2	0.1	5	0.08068	1.55554	0.08061	1.55543
5	0.1	5	0.07339	1.59790	0.07345	1.59831
10	0.1	5	0.03857	1.72927	0.03868	1.72928
5	1	5	0.14754	1.69136	0.14756	1.69136
5	10	5	0.15475	1.71223	0.15498	1.71222
5	100	5	0.15543	1.71441	0.15565	1.71438
5	∞	5	……	……	0.1557	1.71462
5	0.1	10	0.06466	2.39211	0.06468	2.39196
5	0.1	15	0.05710	2.98988	0.05999	2.98993

Table 2: Effects of Pr, k on Temperature profile θ (0) and nanoparticle concentration φ (0), when R = 1, M = 1.5, θ_w = 0.02, Bi = 0.01, Nb = 1

	Values				
Parameters	1	2	3	4	5
Pr =	0.5	1	3	5	10
k =	1.5	1.5	2.5	2.5	3
θ (0) =	0.0096	90.0096	70.0094	40.0090	50.00635
φ (0) =	1.2263	21.2263	21.2263	21.2263	21.22632

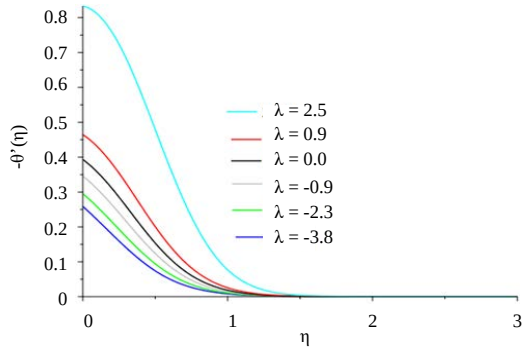

Fig. 2: Heat source influence on the Nusselt number profile

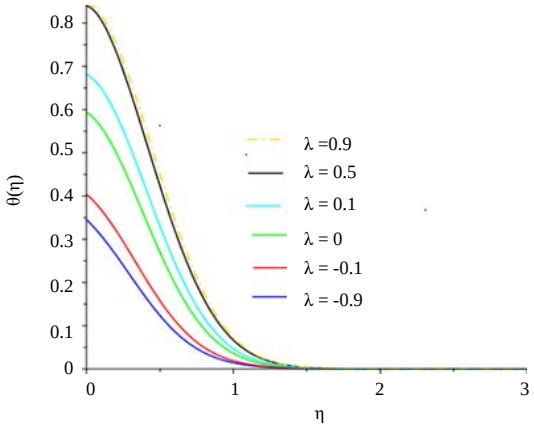

Fig. 3: Heat source influence on the temperature profile

flow model for the above coupled non-linear ordinary differential equations Eq. 6-9 with respect to their boundary conditions Eq. 10 in maple 2020 for different values of governing parameters viz. Prandtl number Pr, radiation parameter R, a Brownian motion parameter Nb, a thermophoresis parameter Nt, Magnetic parameter M, chemical reaction k and a Lewis number Le. The numerical solutions are obtained for velocity, temperature and concentration profiles for different values of governing parameters. The obtained results are displayed through graphs Fig. 2-13 for Nusselt number, Sherwood number, velocity, temperature and concentration profiles, respectively. The accuracy of our result is displayed in Table 1, at the various values of governing parameters involved while considering the heat generation/absorption parameter λ = 0. Thus, a very fascinate agreement between the present and previous studies was attained.

The results displayed in Table 2 shows the effects of Pr, Le on reduced Nusselt number and reduced Sherwood number. It can be observed in Table 2 that, we have presented the impact caused by both Prandtl number and Lewis number on the dimensionless heat transfer rate -θ'(0) with Pr and Le at different values. This resulted in the decrease in the reduced Nusselt number Nur significantly. The dimensionless mass transfer rate -φ'(0), notably increases with Pr and Le at different values. Moreover, increase in the values of Prandtl number and chemical reaction decreases the temperature gradient, where it is noticed that the rate of heat transfer enhances significantly. While the concentration remains constant for whatever values of Pr and k is depicted on Table 3.

Figure 2 shows the effect of Heat generation/absorption on the Nusselt number. The fluid Nusselt number is physically rising in the case of heat

Table 3: Effects of Pr, k on temperature profile θ (0) and nanoparticle concentration φ (0), when R = 1, M = 1.5, θ_w = 0.02, Bi = 0.01, Nb = 1

	Values				
Parameters	1	2	3	4	5
Pr =	0.5	1	3	5	10
k =	1.5	1.5	2.5	2.5	3
θ (0) =	0.0096	90.0096	70.0094	40.0090	50.00635
φ (0) =	1.2263	21.2263	21.2263	21.2263	21.22632

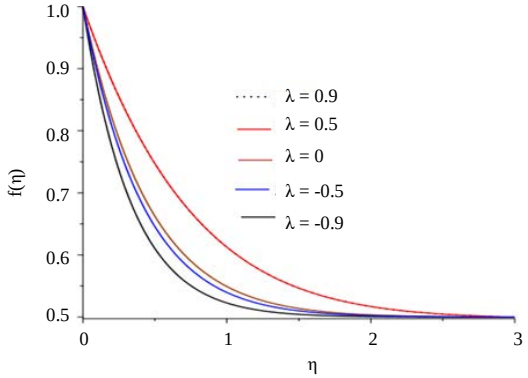

Fig. 4: Heat source influence on velocity profile

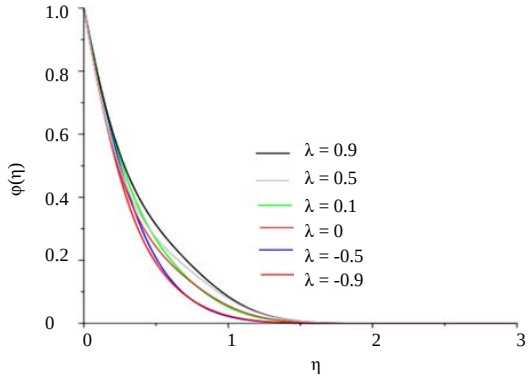

Fig. 5: Heat source influence on nanoparticle concentration profile

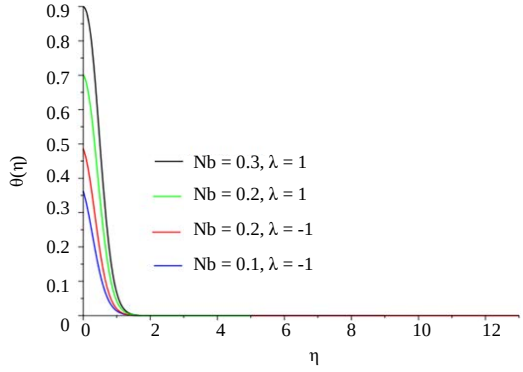

Fig. 6: Effects of Brownian motion (Nb) to the temperature profile θ

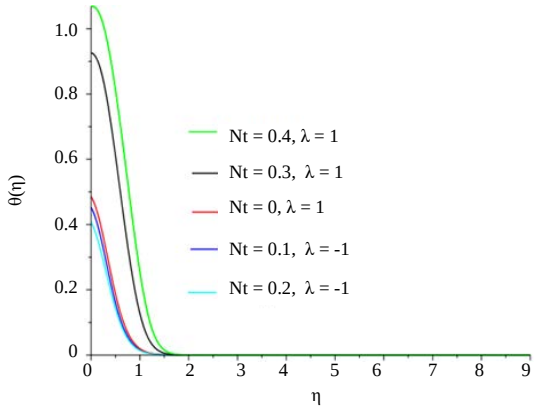

Fig. 7: Effects of thermophoresis (Nt) to the temperature profile θ

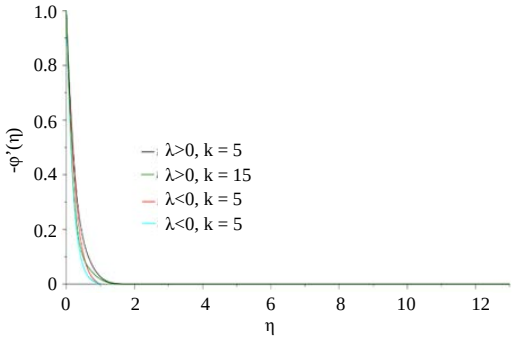

Fig. 8: Effects of chemical reaction (k) to the Sherwood number profile

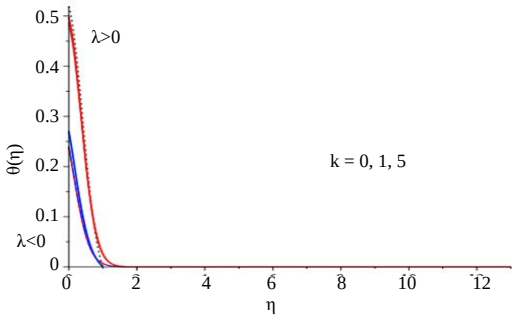

Fig. 9: Effects of chemical reaction (k) to the temperature profile

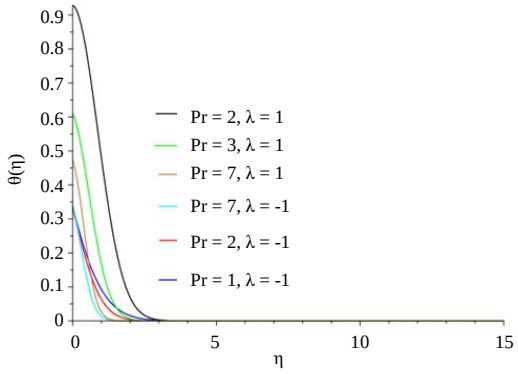

Fig. 10: Effects of Prandtl number (Pr) to the temperature

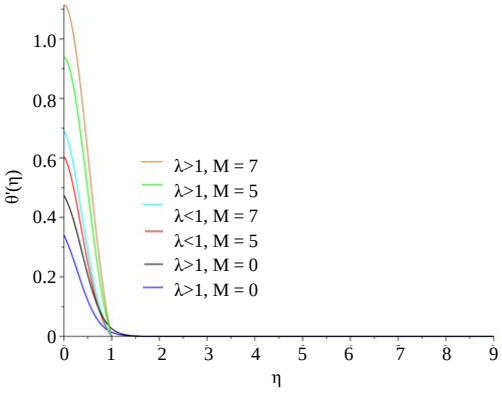

Fig. 11: Effects of Magnetic parameter (M) to the temperature

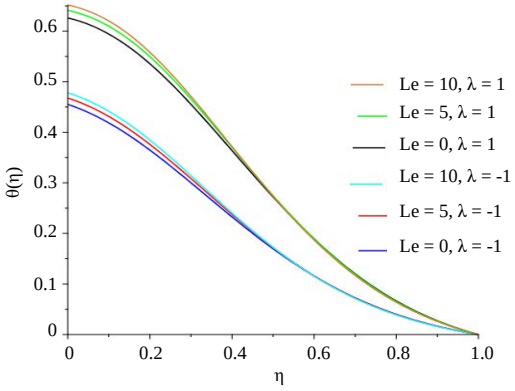

Fig. 12: Effects of Lewis number (Le) to the temperature profile

generation (λ>0) and decreases in the case of heat absorption (λ<0), respectively. Also Fig. 3 shows the effects of heat generation/absorption on the temperature profile. The fluid's temperature is physically rising with the increment in both heat generation (λ>0) and heat absorption (λ<0), respectively. It is clear from Fig. 4, that

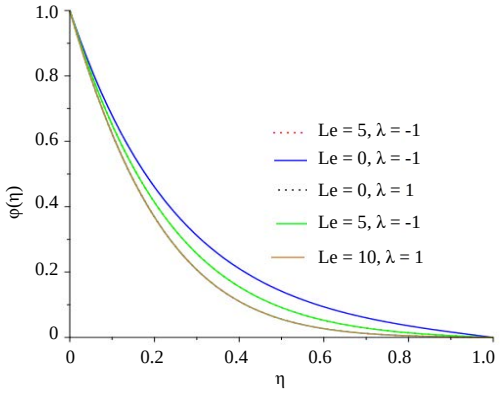

Fig. 13: Effects of Lewis number (Le) to the nanoparticle concentration profile

the fluid's velocity is physically increases in both cases of heat generation (λ>0) and heat absorption (λ<0), respectively. It can be seen from Fig. 5, that the fluid's concentration is increasing irrespective of heat generation (λ>0) and heat absorption (λ<0).

With regard to Fig. 6 increasing the value of Nb increases the temperature with heat generation (λ>0) while increasing the value of Nb decreases the temperature in the case with heat absorption (λ<0), respectively. It can be well observed that in Fig. 7 increase in the values of Nt leads to the drastic increase in the temperature profile with respect to heat generation (λ>0). But it decreases with increase in the values of Nt with respect to heat absorption (λ<0) along with the stretching sheet. Irrespective of heat generation (λ>0) or heat absorption (λ<0), the Sherwood number increases with the increase in the values of k on Fig. 8.

Figure 9 depicted the following with heat generation (λ>0) the temperature rises with the increase in the values of k, similarly with heat absorption (λ<0) also the temperature rises with the increase in the values of k on Fig. 10. It is found that with heat generation (λ>0): increase in the value of Pr drastically decreases the temperature. Whereas, with heat absorption (λ<0): for any value of Pr the temperature remain constant. At M = 0: the temperature increase with heat generation (λ>0) and it decreases with heat absorption (λ>0). Furthermore, increase in the value of M for any non-zero value (M>0) yield an increase in the temperature for both heat generation (λ>0) and heat absorption (λ<0) as on Fig. 11. Increasing the value of Le rises the temperature drastically with heat generation (λ>0) and it decreases with decreasing the value of Le with heat absorption (λ<0) on Fig. 12. The nanoparticle concentration rises irrespective of heat generation (λ>0) or heat absorption (λ<0) (Fig. 13).

CONCLUSION

In this study, the influence of heat generation/absorption parameter has been studied, along with other pertinent parameters such as chemical reaction k, Brownian motion parameter Nb, thermophoresis parameter Nt, Prandtl number Pr, Lewis number Le and magnetic parameter M on the flow field and natural convective boundary layer flow of a nanofluid past a stretching sheet in the presence of heat generation/absorption. The analysis to this problem was made numerically. Our results found to be in good agreement with the previous study by Madaki *et al*.[10] while some distinct parameters in this study being limited to zero. The results found in this study can be summarized as follows: the fluid Nusselt number is physically rising in the case of heat generation ($\lambda>0$) and decreases in the case of heat absorption ($\lambda<0$), respectively. The fluid temperature is physically rising in the case of heat generation ($\lambda>0$) and decreases in the case of heat absorption ($\lambda<0$), respectively, fluid's velocity is physically rising in both cases of heat generation ($\lambda>0$) and heat absorption ($\lambda<0$), respectively, increase in the value of heat generation/absorption rises nanoparticle concentration profile rapidly, increasing the value of Nb increases the temperature with heat generation ($\lambda>0$) while increasing the value of Nb decreases the temperature in the case with heat absorption ($\lambda<0$) respectively. 6)increase in the values of Nt leads to the drastic increase in the temperature profile, with respect to heat generation ($\lambda>0$). But it decreases with increase in the values of Nt with respect to heat absorption ($\lambda>0$) along with the stretching sheet. Irrespective of heat generation ($\lambda>0$) or heat absorption ($\lambda<0$), the Sherwood number remain constant for all the values of k. At M = 0: the temperature increase with heat generation ($\lambda>0$) and it decreases with heat absorption ($\lambda<0$). Furthermore, increase in the value of M for any non-zero value ($M>0$) yield an increase in the temperature for both heat generation ($\lambda>0$) and heat absorption ($\lambda<0$). It is found that with heat generation ($\lambda>0$): increase in the value of Pr drastically decreases the temperature. Whereas, with heat absorption ($\lambda<0$): for any value of Pr the temperature remain constant. At M = 0: the temperature increase with heat generation ($\lambda>0$) and it decreases with heat absorption ($\lambda<0$). Furthermore, increase in the value of M for any non-zero value ($M>0$) yield an increase in the temperature for both heat generation ($\lambda>0$) and heat absorption ($\lambda<0$). Increasing the value of Le rises the temperature drastically with heat generation ($\lambda>0$) and it decreases with decreasing the value of Le with heat absorption ($\lambda<0$). The nanoparticle concentration rises irrespective of heat generation ($\lambda>0$) or heat absorption ($\lambda<0$).

NOMENCLATURE

A = Sisko fluid parameter
Nt = Thermophoresis parameter
a, b = Material constants of the fluid
Nd = Modified Dufour parameter
q_r = Radiative heat flux
B_0 = Magnetic field strenth
Nu = Local Nusselt number
C = Solutal concentration
Pr = Prandtl number
C_∞ = Free stream concentration
Nb = Brownian motion
C_w = Skin friction coefficient
Re = Local Reynolds number
Sh = Local Sherwood number
C_w = Nanoparticles volume fraction at the wall
Sh = Nanofluid Sherwood number
φ = Dimensionless solutal concentration
T = Temperature of the fluid
T_w = Temperature of the fluid at the wall
Ec = Eckert number
D_B = Brownian diffusion coefficient
U_∞ = Free stream stagnation point velocity
D_T = Thermophoretic diffusion coefficient
u = Velocity component in x-direction
F' = Dimensionless velocity
v = Velocity component in y-direction
Le = Lewis number
u_w = Stretching sheet velocity
x = Direction along to the plate
y = Direction perpendicular to the plate
n = Power law index
M = Magnetic parameter or Joule heating parameter
α = Fluid thermal conductivity
ρ_f = Density of the fluid
η = Similarity variable
σ = Electrical conductivity of fluid
θ = Dimensionless temperature of the fluid
φ_w = Free stream nanoparticle volume fraction
φ = Dimensionless nanoparticle volume fraction
Ψ = Stream function
k = Thermal conductivity of the fluid
τ = Ratio of the effective heat capacity of the nanoparticles and heat capacity of the fluid

REFERENCES

01. Choi, S.U.S., 1995. Enhancing Thermal Conductivity of Fluids with Nanoparticles. In: Developments and Applications of Non-Newtonian Flows, Siginer, D.A. and H.P. Wang (Eds.). American Society of Mechanical Engineers, New York, pp: 99-105.

02. Mushtaq, A., M. Mustafa, T. Hayat and A. Alsaedi, 2014. Nonlinear radiative heat transfer in the flow of nanofluid due to solar energy: A numerical study. J. Taiwan Inst. Chem. Eng., 45: 1176-1183.
03. Aziz, A., W.A. Khan and I. Pop, 2012. Free convection boundary layer flow past a horizontal flat plate embedded in porous medium filled by nanofluid containing gyrotactic microorganisms. Int. J. Therm. Sci., 56: 48-57.
04. Madaki, A.G., R. Roslan, M.S. Rusiman and C.S.K. Raju, 2018. Analytical and numerical solutions of squeezing unsteady Cu and TiO2-nanofluid flow in the presence of thermal radiation and heat generation/absorption. Alexandria Eng. J., 57: 1033-1040.
05. Pal, D. and G. Mandal, 2020. Magnetohydrodynamic stagnation-point flow of Sisko nanofluid over a stretching sheet with suction. Propul. Power Res., 9: 408-422.
06. Khazayinejad, M., M. Hatami, D. Jing, M. Khaki and G. Domairry, 2016. Boundary layer flow analysis of a nanofluid past a porous moving semi-infinite flat plate by optimal collocation method. Powder Technol., 301: 34-43.
07. Mabood, F., W.A. Khan and A.M. Ismail, 2015. MHD boundary layer flow and heat transfer of nanofluids over a nonlinear stretching sheet: A numerical study. J. Magn. Mater., 374: 569-576.
08. Animasaun, I.L., 2015. Effects of thermophoresis, variable viscosity and thermal conductivity on free convective heat and mass transfer of non-darcian MHD dissipative Casson fluid flow with suction and nth order of chemical reaction. J. Niger. Math. Soc., 34: 11-31.
09. Kasmani, R.M., S. Sivasankaran, M. Bhuvaneswari and Z. Siri, 2016. Effect of chemical reaction on convective heat transfer of boundary layer flow in nanofluid over a wedge with heat generation/absorption and suction. J. Appl. Fluid Mech., 9: 379-388.
10. Madaki, A.G., D.G. Yakubu, M.Y. Adamu and R. Roslan, 2019. The study of MHD nanofluid flow with chemical reaction along with thermophoresis and Brownian motion on boundary layer flow over a linearly stretching sheet. J. Pure Applied Sci., 19: 83-91.